CHALLENGES TO WAVE HINDCASTING IN THE CASPIAN SEA

C. Graham[1], V. J. Cardone[2], E. A. Ceccacci[2], M.J. Parsons[2], C. Cooper[3], J. Stear[3]

[1]Shell International
Rijswijk, Netherlands

[2]Oceanweather
Cos Cob, USA

[3]ChevronTexaco
San Ramon, USA

1. INTRODUCTION

The recent discovery in the very shallow waters of the northern Caspian Sea of arguably one of the world's last giant oil accumulations, and ongoing exploration and production activities over this basin as a whole, have created an urgent need for reliable normal and extreme wind, wave, surge and current climate data. Many problems peculiar to this basin pose significant challenges to the routine application of the hindcast method to establish the metocean climate descriptions needed for engineering designs. The northern area is covered by ice in winter; air temperature extremes range from minus 36°C to plus 40°C, winds can exceed Force 12, and in the operationally significant shallow water areas (averaging just 4 m), the storm driven water level anomaly can be up to plus/minus 2 m making it necessary to account for such changes in the wave modeling. To make matters worse, even the still water level of the basin has undergone significant and poorly understood multi-decadal secular changes of up to 2 m over the past century. Finally, the lack of conventional marine data makes specification of wind fields more difficult than in typical open basins and marginal seas.

This paper describes how these challenges were overcome as part of a comprehensive hindcast study of the basin (CASMOS, for CAspian Sea MetOcean Study). CASMOS utilized a 3G wave model adapted on a 10-km grid system and hydrodynamic modeling at comparable resolution to hindcast storm periods and a continuous period. The hindcast extended to 100 storms over a 52-year period 1948-2000 and to the 10-year continuous period 1991-2000. The study tapped western meteorological data sources as well as the resources of the Azerbaijan Hydrometeorological Center, the Kazakhstan KAZHydromet Office and the Russian World Data Center. Nevertheless, it was necessary to utilize QuikSCAT data to identify systematic errors in surface winds observed at coastal stations and NCEP Reanalysis products before accurate surface wind fields could be derived. A successful validation of waves, currents and surge was made in the shallow northern area utilizing the results of recent measurement programs. However, the friction factor of the 3G wave model had to be increased over that of official WAM to achieve minimum bias.

The need for CASMOS was determined by members of the OGP (Oil & Gas Producers) Metocean Committee in the late 1990's with the objective of establishing definitive metocean design criteria and operational planning statistics to support a wide range of activities including:

(a) design of offshore structures, islands and pipelines;
(b) installation and operation of offshore facilities,
(c) logistics, marine operations, aviation;
(d) coastal engineering projects, such as shore terminal design and operation;
(e) database for environmental assessment and impact studies.

CASMOS was formed with five participants under the project management of Shell. Oceanweather (OWI) was responsible for data assembly, wind and wave modeling and the integration of wind and wave hindcast products with hydrodynamic model hindcasts, whilst the 2-D and 3-D hydrodynamic modeling was carried out by ChevronTexaco. The study built upon an earlier proprietary hindcast study of the Azerbaijan sector carried out in 1996 by OWI for the AIOC consortium.

2. CLIMATE AND OCEANOGRAPHY OF THE CASPIAN SEA

The Caspian Sea (Figure 1) extends approximately 1,200 km from north to south, with an average width of 325 km east to west, covering a total area of some 400,000 km^2 (Kosarev et al, 1994). As of 1995, the mean sea level was 26.6 m below Baltic datum, equivalent to global mean sea level (CEP, 1999). Most of the northern Caspian is shallow, with water depths averaging only 4 m. The central Caspian approaches depths of 800 m, while the southern Caspian has a maximum depth of slightly over 1000 m.

The climate of the Caspian region varies substantially from north to south. In the south, summers are hot and dry, and winters are warm. In the north, the summers are similar to the south, but the winters often bring storms with gale-force winds and significant variations in temperature. During the winter, weather in the northern Caspian is dominated by the Asiatic anti-cyclone which creates easterly winds of cold, clear air. During the summer, the weather is dominated by the Azores high-pressure that causes northerly winds. The region is subject to extratropical cyclones (Sovintervod, 1993) at the rate of about 10 storms per year. These approach from the west, southwest or south, although a significant number are also generated locally. Cyclones most often appear in January, March and October. During the winter, arctic air mass intrusions frequently affect the northern Caspian, bringing cold, snow and strong north winds.

With the climatic differences between the northern and southern Caspian, the non-summer distribution of water temperatures is several °C between the major basins in the upper water column. Vertical thermal differences, however, are small during most of the year. As summer approaches, temperatures become more uniform across the entire sea. A strong thermocline develops in the top 20 to 40 m of the deeper portions of the central and southern Caspian in mid-summer, and persists into early fall. Salinity in the Caspian is almost three times lower than that found in the open ocean, with an average of about 12.8 psu. The lowest salinity is found in the northern Caspian, where there is a large inflow of fresh water from the Volga and Ural rivers. Ice forms in the northern portions of the Caspian in early November and reaches its maximum southward extension by January or February. The long-term decadal fluctuation of water level over the last 100 years has been more than 2 m (Figure 2). An explanation of the various factors influencing this fluctuation may be found in Kosarev et al, (1994).

3. DATA SOURCES AND TYPES

A variety of data sources and data types were utilized for this study. The key sources are summarized below:

Azerbaijan Hydrometeorological Service (AHS) have lists of dates of significant storms, hand analyzed (isobars) 6-hourly surface weather maps in storms with station data plotted, tabulations of surface weather observations in storms for selected stations, and maps of the maximum ice extent in storms. Data were provided for 23 events, mainly drawn from the late 1940s, 1950s and 1980s.

Russian World Data Center, Obninsk (WDC) and St. Petersburg, provided a historical storm list, 6-hourly (3-hourly) objectively analyzed maps of surface pressure (wind) in selected storms, ASCII files of digitized versions of the above, ice maps for storms and continuous periods and annual Caspian Sea water level fields for the years 1945 – present. These products (except water levels) were provided for 20 events within the 11-year period 1966-1976.

KazHydromet, Almaty (KHI) provided, via ChevronTexaco, a historical storm listing for the northeastern Caspian Sea, digitized files of surface weather observations for Peshnoy, Tyuleny and Kulaly 1946-1990, and water level at selected stations in storms. Also obtained were digital files of surface observations from Aktau and Dubendi for the period 1988 to 1997.

US NOAA National Climatic Data Center, Asheville (NCDC). Relevant historical data utilized include the Northern Hemisphere Surface Analysis-Final Analysis series on microfilm, which extends from 1954-present, and the TDF-11 ship report files on magnetic tape. However, specifically for CASMOS, OWI had NCDC search its archives for recorded GTS interceptions of surface weather observations from stations surrounding the Caspian Sea in digital form in DATSAV format. A surprising amount of data was found and acquired. In general, three-hourly observations at 12 stations surrounding the Caspian Sea were found for the period 1932-2000, with of course shorter periods at some stations and gaps in others.

NOAA/NCAR 40-Year Reanalysis Project (NRA) database of 6-hourly surface pressure and wind fields covering the globe (Cox et al, 1998) were used as background winds for the continuous hindcasts and to aid in storm screening and selection. The NRA pressure fields were also used to compute an alternative file of surface winds derived via pressure to wind (PRESTO) transformation using Cardone's (1969) marine planetary boundary model.

Satellite Altimeter Significant Wave Height and Wind Speed Estimates from the GEOSAT, TOPEX, and ERS1/2 missions.

Surface wind estimates from the scatterometer on QuikSCAT have been made on a global basis since July 1999. For CASMOS, the 25-km resolution Level 2B data was obtained from NASA's Jet Propulsion Laboratory (JPL). Coverage is excellent over the Caspian Sea with typically two passes per day, often covering the entire basin.

Oceanweather's GROW Database from a 40-year global wave hindcast, recently updated as described in Cardone *et al.*, (2000).

In-Situ Measurements of winds, waves, water level and currents collected in the northern Caspian area were used for model validation purposes, as were currents from a limited program in the Azeri sector. The data are proprietary and limited in extent.

Published Data: A large number of Russian and English language papers, technical reports, atlases, books and compilations of climatological data were referred to.

Ice Data: The approach taken in the hindcasts was to assume basically that the climatology of ice cover in the Caspian Sea, during potentially ice-free periods, and the storm climatology are uncoupled. Therefore, all wave and hydrodynamic model hindcasts were made with a specification of ice corresponding to "minimum ice" for the month. The specification of minimum ice was taken from hard copies of maps supplied by ChevronTexaco.

Water Depth Data for the Caspian were supplemented with the latest available charts and some limited recent sounding data acquired in the northern Caspian area.

4. WAVE AND WIND HINDCAST METHODOLOGY

4.1 Wave Model

OWI's standard UNIWAVE spectral wave hindcast model package, incorporating shallow water processes, was used for all the CASMOS hindcasts. This package has the option to use either the highly calibrated second generation source term physics (ODGP2) or the third generation (3G) physics (OWI3G/DIA2). Further model details may be found in Cardone *et al*., (1989); Swail *et al*., (1992); Cardone and Ewans, (1992); Eid *et al*., (1992).

OWI has developed and tested its own version of the 3G WAM model (WAMD1, 1988) and has achieved excellent results with this model in both tropical and extratropical settings. For many

practical applications though, wind fields are simply not accurate enough to justify the application of WAM or OWI3G over OWI's already skillful ODGP2 model, as described in a recent study of the "Halloween Storm" and the "Storm of the Century" in the early 1990's off the East Coast of North America (Cardone *et al*., 1996). All the models use a common propagation system which is energy conserving, faithfully simulating great circle wave propagation paths and which provides accurate predictions of swell even after propagation distances of over 5,000 miles (Cardone *et al*., 1995). Further validations of the models in long term hindcast studies may be found in Swail and Cox (2000) and Cox and Swail (2001), and for West Africa in Cardone *et al.* (1995).

UNIWAVE was adapted to Caspian Sea on a single-nest system high-resolution grid with the following attributes:

Grid spacing:	0.090 deg Lat by 0.1120 deg Long;
Number of live points:	4078;
Spectrum resolution:	23 frequencies by 24 directions
Physics:	2G (ODGP2) shallow water version or 3G (OWI3G/DIA2) shallow water version
Propagation:	first order interpolatory, refraction and shoaling included
Growth time step:	0.25 hours
Propagation time step:	0.125 hours
Wind input time step:	0.25 hours
Archive time step pickup file:	0.50 hours

Figure 1 shows the wave model grid system and the minimum ice extent for the month of January. In CASMOS, the storm hindcasts were run with the 3G variant of UNIWAVE while ODGP2 was used for the continuous hindcast. The only "tuning" of the wave models made was in the bottom friction source term. In the 3G model, this was accomplished by selecting the friction coefficient of the quadratic friction dissipation source term, which is considered a rather arbitrary factor, to minimize the bias in a validation hindcast. In ODGP2, which uses a more elaborate bottom friction model than OWI3G, the friction was tuned through the bottom sediment sand grain size. For both models, the downstream interpolation propagation scheme as described by Greenwood *et al.* (1985) was used throughout.

4.2 Specification of Water Depth for Wave Model Hindcasts

Three issues needed to be addressed to specify the water depth field for the wave hindcasts:

(a). Determining the nominal water depth at each of the wave model grid points:

The starting input was available sounding and chart depth data. The gridded depths were derived by averaging depths inside each 10 km grid box to provide a depth for the center grid point. In the earlier proprietary Azerbaijan study for the AIOC consortium, this step often yielded boxes with no soundings and the process was extended to averaging over arrays of 3x3 or if necessary 5x5 grid boxes. Unfortunately this process could unduly smooth the bottom in some critical areas, So in CASMOS, if the nominal box average did not yield a depth, values were derived from hand analysis of the depth contours in the locality of each offending area.

The limiting water depth for shallow propagation and growth processes is taken according to the conventional definition: $kd > \pi$, where $k = 0.006123\ m^{-1}$ for the 0.039 Hz frequency bin. Thus, propagation by depth-dependent ray tracing is executed at points within 20 km in any direction of points with depths 513 m or less. In the earlier Azerbaijan hindcast study, the minimum depth allowed at any grid point was 7.5 m. Since the water depth in the north Caspian is very shallow (average 4 m), a number of sensitivity hindcasts were made with both the 2G and 3G versions of the wave model to explore the minimum depth tolerated before instabilities would set in. These runs had a surprising beneficial result of serving as an effective quality control on the gridded depth field and the underlying source of soundings, as almost all apparent "instabilities" in the runs could be traced back to

erroneous soundings that had introduced spuriously large gradients in water depth. This led to an extensive process of "cleaning" of the sounding file and ultimately to a "nominal" gridded depth field which could be used with either the 2G or 3G wave model physics options with minimum depth as shallow as 2 m.

(b) Accounting for the long-term decadal fluctuation in water level of the Caspian Sea.

This fluctuation has been more than 2 m over the last 100 years (Figure 2). The CASMOS steering committee ultimately decided to adopt the peak 1995 reference water level for all storm and continuous wave hindcasts, as well as for the hydrodynamic hindcasts. The secular change in water depth between this reference level and the effective time reference of the sounding file utilized to develop the gridded depth field was estimated to be +1.4 m, so this was added to the depth at all grid points. The seasonal variation of water level in the Caspian Sea was ignored because this source of variability was considerably smaller than even the small natural variation (noise level) of the soundings within a model grid 10-km grid box with respect to the nominal grid point depth.

(c). Accounting for the modulation of the water level in each storm by the storm driven storm surge:

The ideal solution would be to fully couple the wave and hydrodynamic models for the storm hindcasts, but this approach was considered too elaborate to be considered within the time and resource constraints of CASMOS. The original hope was to define typical peak positive surge patterns in a very approximate way by using the hydrodynamic model hindcasts of a few storm scenarios (for example, predominantly northerly, southerly, westerly and easterly "storms") to define typical peak positive storm surge patterns in the Caspian Sea. A more rigorous approach proved necessary. After the wind fields were developed for each historical storm, the 2-D hydrodynamic model was run on each storm by ChevronTexaco. Then for each storm, a file of time histories of the surge at each model grid point was transmitted to OWI where a field of the peak positive surge at each point was formed. That field was then added to the nominal (1995) water depth field before the wave model was run for the storm.

4.3 Wind Field Analysis

All winds were referenced to the average "effective neutral wind speed" at 10-meter height (Cardone, 1969; also Cardone *et al*., 1990), a virtual wind speed which has been widely accepted by the ocean response and remote sensing communities. A flow chart of the overall CASMOS hindcast methodology (Figure 3) shows the wind field data sources feeding into the interactive kinematic objective analysis process method (Cox *et al*., 1995) to develop the surface wind fields. The same methodology was used to develop for both the storm and continuous wind fields, but a greater amount of time per 6-hour analysis was spent on the storm fields. Input to the system consisted of background wind fields from the 6-hourly 10-m surface wind fields in the NCEP/NCAR Reanalysis Project (NRA) and meteorologist input in terms of kinematic control points for each analysis. Given the lack of any *in-situ* wind measurements in the Caspian Sea, even from transient ships, it was necessary to transform all data sources to effective over-water exposure using the recently acquired QuikSCAT data set. The following data were processed in this manner:

(a) *QuikSCAT vs. The NOAA/NCEP surface wind fields available at approximately a 2 degree grid*

The QuikSCAT (Q/S) data consist of individual 25-km wind vector cells from the period July 1999 to January 2001, after filtering for land, ice and rain using flags in JPL Level 2B data file. Passes are near 0200 GMT (5AM local) and 1500 GMT (6PM local). The NRA gridded winds are available 6-hourly, on a 2-degree grid. To produce an overlapping Q/S NRA data set, the NRA wind fields were interpolated linearly to hourly intervals and matched temporally and spatially with the Q/S data. OWI's TIMESCAT program was then applied to the overlapping data sets to provide standard difference statistics on wind speed and direction based on individual data pairs, as well as distributional comparisons of wind speed in terms of quantile-quantile scatter plots. The linear regression through

the q-q plot served as the transformation. The analysis was carried out on the following data stratifications:

- Two “seasons” defined as October – March and April – September
- Four wind direction quadrants centered on NRA wind directions North, East, South and West
- Three broad regions defined as Northern, Central and Southern Caspian Sea

It was found necessary to filter Q/S winds > 22 m/s in the central region for southerly directions because those data were apparently contaminated by rain. After considerable experimentation, the final regressions were defined, and then evaluated as corrections of fictitious steady-state wind fields.

(b) *QuikSCAT vs. Synoptic observations from land stations*

A similar analysis was carried for each land station that had data for the period of the Q/S mission. The land station data at 10 stations are 3-hourly with many gaps. The observations were interpolated to 1-hourly and matched with Q/S data that fell within boxes around each station. The boxes were of different dimensions depending on station location, but usually about 1 x 2 degrees. Because of very poor correlations, two stations were dropped (Babulsar and Lenkoran) suggesting that the measured data had very little value to indicate the over water wind. The seasonal stratifications were also dropped but a stratification on synoptic hours (02GMT and 15GMT) was retained to try to capture diurnal effects. After considerable experimentation, final regressions were defined.

(c) *QuikSCAT vs. “PRESTO” Winds computed from NOAA/NCEP pressure gradients and air-sea temperature on a 2.5 degree grid*

A separate analysis was carried out on winds (PRESTO) computed from NRA pressure gradients, because some of our recent studies have suggested that the pressure gradients may be specified more accurately than the wind fields. For some regimes in the Caspian Sea, the surface flows are highly ageostrophic and accelerated for certain imposed pressure fields. If the physics of the NRA model does not capture these effects, but Q/S observes them, it may be possible to develop useful transformations for such regimes from the PRESTO winds. The Presto wind fields were computed 6-hourly on a 2.5-degree grid, yielding just five (5) data points over the entire Caspian Sea. These winds were interpolated to hourly intervals and matched with Q/S data within either 1 x 1.5 degree (latitude x longitude) or 1 x 2 degree (along 40° N) boxes. The data stratifications selected for the analysis of PRESTO winds were the same as used for the NRA winds.

5. WAVE HINDCAST VALIDATION

Considering the level of offshore development in recent years in the Caspian Sea, there is remarkably little *in-situ* measured wave data available to validate model hindcasts. The study focused on proprietary measurements collected in 2000 in the shallow waters of the northern Caspian. Considering the extensive and very successful validation of the wave models in deep water areas made in previous studies, this validation provided the opportunity to specifically tune the shallow water dissipation source terms for unbiased hindcasts in an area of the Caspian that is of particular interest to the oil & gas industry. A total of six wave model runs were made:

- ODGP2 with nominal sediment (i.e. sand grain size), nominal grain/4, and with nominal grain x 2.
- OWI3G52 with nominal WAM friction, half nominal friction, and with twice nominal friction.

The statistics of the differences between measured and hindcast wave height and period at two grid points showed that the runs with the greater friction produced the least bias (Figure 4). OWI3G with twice friction was used for all storm hindcasts and ODGP2 with twice grain size was used for the 10-year continuous hindcast.

6. PRODUCTION WAVE HINDCASTS

6.1 Selection of Storm Population

The following sources of information were utilized to yield a target representative population of 100 storms for hindcasting:

- List of 33 storms, mainly of the northwesterly type, drawn up for the earlier Azerbaijan study.
- List of storms, producing water level anomalies in the shallow waters of the northern Caspian, drawn up by ChevronTexaco for modeling exercise associated with their Tengiz development;
- OWI's GROW (1958-1999) and GROW2000 (1970-1999) global hindcasts;
- OWI's file of 6-hourly PRESTO winds computed from the NRA;
- Time series of observed surface winds in synoptic coastal station observations;
- Time series of coastal station synoptic sea level pressure differences for various sections across the Caspian Sea.

From the above and after consideration of the general synoptic climatology of Caspian Sea storms, the following 100 storms were selected from the period 1948 to 2000:

- 33 "northerly" events affecting most areas of the Caspian Sea
- 30 storms of the "south" and "southwest" type
- 5 "easterly" events and 10 new "westerly" events in the northern area
- 10 "easterly," 5 "westerly" and 7 "northerly" events in the central/southern areas

The directionality above refers to the approximate orientation of the wind direction (from which) along the fetch of predominant peak wave generation in a storm, though it is not uncommon for one historical event to be comprised of two or more types affecting different parts of the Caspian Sea. The meteorological synoptic patterns responsible for the generation of storms are quite varied and include eastward propagating extratropical storms, cyclone redevelopment within the Caspian Sea, strengthening of southerly pressure gradients in advance of eastward propagating fronts, strong outbursts of cold air behind cold fronts, tightening gradients over the Caspian Sea between quasi-stationary pressure systems and others. There have been some references in the Russian literature to predominant "weather types" for the Caspian Sea but no attempt was made within CASMOS to develop a more general synoptic climatology of Caspian Sea weather, since our objective was to define the forcing for ocean response models.

6.2 Production Storm Hindcasts

Each of the 100 storms was hindcast with the 3G variant of the CASMOS wave model. However, before each wave run the nominal 1995 reference water depth field was modified to account for the storm surge specified for that storm by the 2-D hydrodynamic model run. The process involved first the extraction from the ChevronTexaco model output the maximum positive surge at each grid point. Then a depth generation program was run with that file to create a depth anomaly grid. The anomaly field was added to the nominal 10 km model grid depth field. The output of each storm run included the usual field analysis parameters archived at 1-hourly intervals at all grid points. Time histories of the 2-D spectra were also saved at 400 grid points for possible use in future fine mesh studies or for site-specific studies requiring spectra. As a quality control measure, each storm "fields" file was processed to compute fields of maximum significant wave height and wind speed, which was then manually viewed.

6.3 Production Continuous Hindcasts

The 10 year period 1991 to 2000 was continuously hindcast using the ODGP2 model, in stovelengths of one month. For the first month spin-up was ignored, while for each succeeding month the hindcast was initialized with a file of restart spectra at each grid point saved from the run of the previous month. The nominal 1995 reference water depth field was used throughout and ice cover was specified as the minimum for each month. The archive produced was identical to that of the storm runs except that

the archive interval was 3-hours instead of 1-hour. As a quality control measure, each monthly “fields” file was processed to compute fields of maximum significant wave height and wind speed, which was then manually viewed. No specific validation of the continuous hindcast was attempted for the basin as a whole, though the runs described in Section 5 above served as a validation at least of the northern shallow water area.

7. WATER LEVEL AND CURRENT MODELING

The hydrodynamic modeling effort was undertaken by ChevronTexaco, drawing upon their earlier 2-D modeling work undertaken for the shallow waters of the northeast Caspian in connection with the Tengiz field development. This earlier work identified the following challenges:

- determining the actual monthly MSL in the northern Caspian is a challenge, with coastal data strongly influenced by river inflow;
- the non-linear coupling between MSL and the surge height is less than 10%, but rises in MSL permit the inundation of areas further inland;
- three to four days of spin-up time are needed to successfully model many of the storm events.

7.1 FEMA Hydrodynamic Model

The hydrodynamic model used was a modified version of the U.S. Federal Emergency Management Agency model (FEMA, 1988). Traditional surge models assume land grid points are effectively cliffs that allow no flooding. The FEMA model though accounts for the flooding and drying of land areas, which is a not-uncommon occurrence in the northeast Caspian where the water’s edge can move inland 20 km or more during a strong eastward-blowing storm.

The model is based on an explicit, two-dimensional, space-staggered finite-difference solution of the shallow-water wave equations. These equations are a simplified form of the continuity equation (conservation of mass) and the Navier-Stokes equations (conservation of momentum). The equations are solved at discrete locations on a rectangular computational grid. The momentum equation represents the balance between inertial forces and gravity forces, wind stress, atmospheric pressure gradient forces, reactive bottom friction forces, and the Coriolis acceleration effect caused by the earth’s rotation. Atmospheric pressure, surface wind stress, bathymetry, bottom friction and other flow resistance coefficients are taken as inputs to the model. The model calculates and outputs the temporal and spatial fields of the 2-D current velocity field and water level (surge).

7.2 Modeling Methodology

A rectangular model bathymetry/land elevation grid was adopted (cell size of 10 km square, 63 cells east to west by 119 cells north to south), covering the entire Caspian Sea. A critical aspect of the Caspian is its fluctuation in water level of 2 m over recent years (Figure 2), as this will have an impact on which areas are subject to flooding when coastal surges occur. The wave and surge/current models were set up using the peak water level in 1995 as the reference level (minus 26.6 m Baltic datum). Much attention was paid to capturing the areas that could potentially flood in the northeast Caspian, as this is a region of particular interest. Most of the remaining coastline was modeled as cliffs, i.e. non-floodable.

As already mentioned, ice forms in the northern portions of the Caspian during fall and winter months. This has significant implications for wind-generated surge and current in the North, as the ice will act to shield the underlying water, and hence act as a moderating influence on current speeds and coastal surges. For the wave and surge/current hindcasts the ice coverage associated with “mild” winters was used, since this is conservative. This confines the presence of ice to the months of January, February and March. For cells with ice coverage, wind stress was set to zero. For the storm analyses, the ice coverage applied to the model was taken to be the coverage for the month in which the storm peak occurred. For the continuous analyses, the model was run in one month increments,

with the inclusion of seven days from the previous month's wind data to ensure proper "spin up" of the model.

The FEMA model itself has been closely scrutinized as it is used by the U.S. Federal government to establish flood insurance rates along the U.S. coastline. It was validated for the Caspian using water level time series from coastal stations and limited propriety offshore water level/current measurements. A number of parameters can be used to fine tune the solution, the most important being changing the bottom friction and ignoring non linear convective terms.

7.3 Model Runs

The FEMA model was run using wind fields supplied by OWI for the 100 storms and 10 year continuous hindcast. The winds used were one-hour average, 10 m elevation (neutral) winds at intervals of three hours. Output was generated of the wind-generated surge (water level) and of the wind-generated 2-D currents (i.e. constant through the water column, depth mean value).

Further work was also undertaken to model and derive the 3-D wind-generated currents for the 100 storms. A number of issues needed to be addressed, not least the fact that the Caspian is unstratified during the cold months – at least half of the year.

8 DERIVATIVE PRODUCTS

The principal product of CASMOS consists of a DVD-ROM and CD-ROM database of all of the storm and continuous hindcast results and derivative products, point sorted, for all grid points in the CASMOS model domain. It comes together with OWI's access and processing software (OSMOSIS) to produce, display and export extreme and normal wind, wave, surge (both positive and negative) and 2-D and 3-D current statistics at user selected grid points. Extremes and normals are also pre-calculated and are available as pre-computed tables. Sample results of the pre-computed tables of extremes are presented in Figure 5.

The 100 year maximum wave height results for the shallow waters of the northern Caspian (model run at 1995 reference level) were somewhat surprising in that it does not appear necessary to invoke a breaking limit to produce design extremes. Apparently, the tuning of the shallow water source term in the OWI3G wave model provides sufficient attenuation of growth to avert an imposition of an external asymptote to growth at these water depths. Another factor in this regard was the finding in some of the model testing, that swell from storm waves generated in the central and southern parts of the Caspian Sea are completely attenuated by shallow water processes in the shoaling waters between 44°N and 45°N. As a result, the wave periods associated with the extreme waves in the northern part of the basin are only between 5 and 6 seconds. This finding is supported at least in anecdotal evidence from the recent drilling programs in the area, which have reported a complete absence of low frequency "swells" in this area.

9 CONCLUSIONS

The CASMOS project has successfully generated a comprehensive set of wind, wave, water level and current data for the whole Caspian Sea basin, for 100 representative storms over a 52 year period, and for a 10 year continuous period. These data will prove invaluable for design and operational planning purposes as the hydrocarbon development of the Caspian advances further.

Modeling the Caspian has presented an unique set of challenges and has produced some interesting results. These are, in summary:

- the complete lack of conventional marine wind data in the Caspian from which to develop wind fields; the quantity of propriety measurements is extremely small;

- the very shallow waters (4 m) in the north Caspian in the vicinity of one of the world's largest oil discoveries in more than 20 years - the Kashagan Field;
- a secular varying depth field with changes of over 2 m over the last 100 years;
- the interaction between the water level (surge) and wave models;
- the small differences (again) found between 2G and 3G wave model approaches;
- there is apparently so much dissipation from bottom friction terms (in both the 2G or 3G wave models) that it was not necessary to apply a parametric wave breaking condition to the computed extremes, even in the shallow waters of the north Caspian area;
- the separation of northern and central Caspian by a sill such that no low frequency wave energy apparently can propagate into the northern part from storms in the south;
- the need to include coastal flooding in the water level (surge) modeling;
- 3-D modeling the Caspian currents and the fact that the Caspian is unstratified for half of the year.

The CASMOS database and study products are confidential to the participants; late participation is possible.

10 ACKNOWLEDGEMENTS

The authors would like to thank the CASMOS participants for permission to publish this paper and for their comments on the paper content. The CASMOS participants are Agip, BP, ChevronTexaco, ExxonMobil and Shell (JIP Project Manager).

11. REFERENCES

Cardone, V. J., 1969: Specification of the wind distribution in the marine boundary layer for wave forecasting. Report TR-69-01, Geophysical Sciences Laboratory. New York University. (Available from NTIS #AD 702-490, 137pp).

Cardone, V. J., D. Szabo and F. J. Dello Stritto, 1989: Development of extreme wind and wave criteria for Hibernia. 2nd Int'l Workshop on Wave Hindcasting and Forecasting, Vancouver, BC, 25-28 April, 1989, 75-88.

Cardone, V. J., J. G. Greenwood, and M. A. Cane, 1990. On trends in historical marine wind data. J. of Climate, 3, 113-127.

Cardone, V. J., 1991: The LEWEX wind fields and baseline hindcast. In: Directional Ocean Wave Spectra. R. C. Beal, Ed., Johns Hopkins University Press, 136-146.

Cardone, V. J. and K. C. Ewans, 1992: Validation of the hindcast approach to the specification of wave conditions at the Maui location off the west coast of New Zealand. Preprints of the 3rd International Workshop on Wave Hindcasting and Forecasting. Montreal, Quebec. May 9-22, 1992; p. 232-247.

Cardone, V. J., H. C. Graber, R. E. Jensen, S. Hasselmann and M.J Caruso, 1995: In search of the true surface wind field during SWADE IOP-1: Ocean wave modeling perspective. The Global Atmosphere-Ocean System., 3, 107-150.

Cardone, V.J., C.K. Cooper and D. Szabo, 1995: A hindcast study of the extreme wave climate of offshore West Africa (WAX). Offshore Technology Conference, 27, paper # 7687, 439 - 451.

Cardone, V. J., R. E. Jensen, D. T. Resio and V. R. Swail, and A. T. Cox, 1996: Evaluation of contemporary ocean wave models in rare extreme events: "Halloween Storm" of October, 1991; Storm of the Century of March, 1993. J. Atmos. and Ocean. Tech., 13, 198-230.

Cardone, V. J., A. T. Cox and V. R. Swail, 2000: Specification of the Global Wave Climate: Is this the Final Answer? 6th International Workshop on Wave Hindcasting and Forecasting. Monterey, California. November 6-10, 2000.

Caspian Environment Programme (CEP), website http://www.caspianenvironment.org/caspian.htm, Baku, Azerbaijan, 1999-2002.

Cox, A.T., J.A. Greenwood, V.J. Cardone and V.R. Swail, 1995: An interactive objective kinematic analysis system. Proceedings 4th International Workshop on Wave Hindcasting and Forecasting, October 16-20, 1995, Banff, Alberta, p. 109-118.

Cox, A.T., V.J. Cardone and V.R. Swail, 1998: Evaluation of NCEP/NCAR reanalysis project marine surface wind products for a long term North Atlantic wave hindcast. Proc. 5th International Workshop on Wave Hindcasting and Forecasting, Melbourne, FL.

Cox, A. T. and V. R. Swail, 2001: A Global Wave Hindcast over the Period 1958-1997: Validation and Climate Assessment. J. of Geophys. Res. (Oceans), Vol. 106, No. C2, pp. 2313-2329.

Eid, B., V. J. Cardone, and V. K. Swail, 1992: Beaufort Sea extreme wind/wave hindcast study. Preprints of the 3RD International Workshop on Wave Hindcasting and Forecasting. Montreal, Quebec. May 9-22, 1992; p. 351-361.

FEMA, 1988: Coastal Flooding Hurricane Storm Surge Model: Methodology. Federal Emergency Management Agency, Federal Insurance Administration, Department of the Interior, United States, Washington, D.C., Vol 1, August 1988.

Greenwood, J. A., V. J. Cardone, and L. M. Lawson, Intercomparison test version of the SAIL wave model, in *Ocean Wave Modeling*, pp 221-233, Plenum, New York, 1985.

Kosarev, A. N., and Yablonskaya, E. A., "The Caspian Sea," SPB Academic Publishing, The Hague, The Netherlands, 1994.

Rodionov, S.N., 1994. Global and Regional Climate Interaction: The Caspian Sea Experience. Water and Science Technology Library, Kluwer Academic Publishers.

Sovintervod, 1993: "The Caspian Sea: Natural Environment, Forecast of Level Fluctuations and Surge Phenomena," proprietary report transmitted to CPTC.

Swail, V. R., V. J. Cardone and B. Eid, 1992: An extremes wind and wave hindcast off the west coast of Canada. Preprints of the 3rd International Conference on Wave Hindcasting and Forecasting, May 9-22, Montreal, Quebec, 339-350. Published by Environment Canada, Downsview, Ontario.

Swail,V.R. and A. T. Cox 2000. Evaluation of NCEP/NCAR reanalysis project marine surface wind products for a long term North Atlantic wave hindcast. To appear in J. of Atmos. And Oceanic Tech.

Schwab, D. J., and Muhr, G. C., 1989: Caspian Sea Project Report. Great Lakes Environmental Research Laboratory, National Oceanic and Atmospheric Administration, Department of Commerce, United States, Ann Arbor, MI, Dec 1989.

WAMDI Group (13 authors, including V. J. Cardone and J. A Greenwood), 1988: The WAM model - a third generation ocean wave prediction model. J. of Phys. Oceanog., 18, 1775-1810.

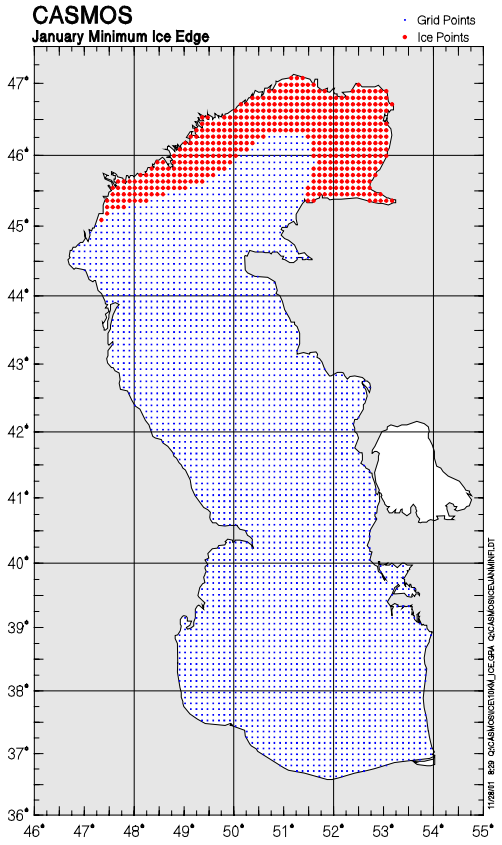

Figure 1. Caspian Sea Grid Map

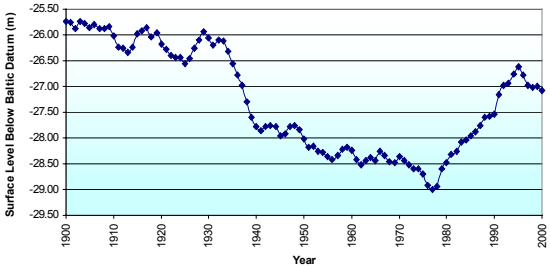

Figure 2. Caspian Sea Water Level Relative Baltic Datum

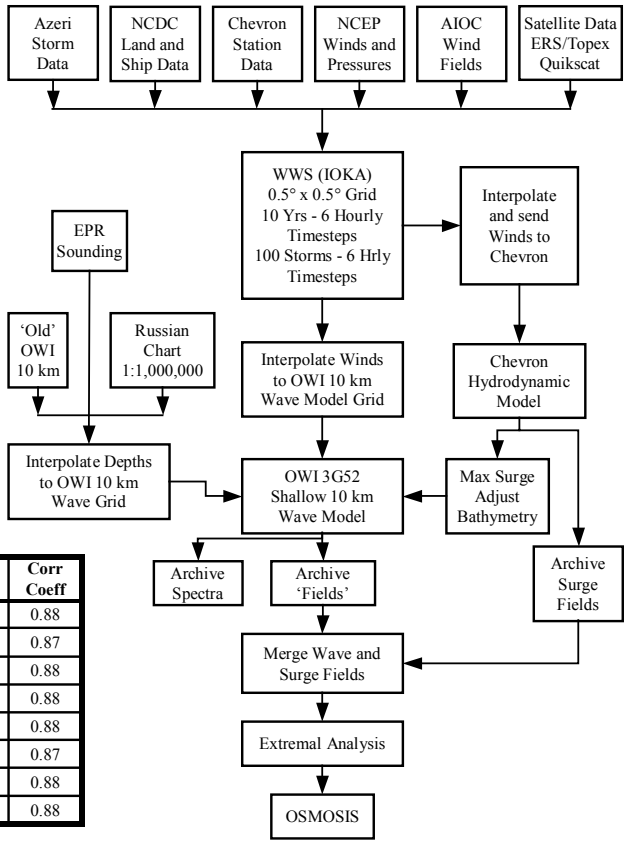

Figure 3. CASMOS Hindcast Methodology

Significant Wave Height (m)

Wave Run	# of Pts	Diff (H-M)	Stnd Dev	Scatter Index	Ratio	Corr Coeff
ODGP2	229	0.11	0.15	0.32	0.76	0.88
ODGP2 (Grain/4)	229	0.11	0.17	0.37	0.76	0.87
ODGP2 (Grainx2)	229	0.12	0.16	0.34	0.77	0.88
ODGP2 (Grainx2) gp 3892	229	0.09	0.15	0.32	0.75	0.88
OWI3G52	229	0.10	0.21	0.45	0.64	0.88
OWI3G52 (F/2)	229	0.26	0.31	0.66	0.73	0.87
OWI3G52 (Fx2)	229	0.06	0.20	0.42	0.60	0.88
OWI3G52 (Fx2) gp 3892	229	0.02	0.19	0.39	0.54	0.88

Figure 4. CASMOS Wave Validation

```
Return Period Extremes for the following fields:
MAXIMUM SIGNIFICANT HEIGHT (m)
MAXIMUM INDIVIDUAL WAVE HEIGHT (m)
MAXIMUM INDIVIDUAL CREST HEIGHT (m)
MAXIMUM WIND SPEED (m/s)
MAXIMUM SURGE HEIGHT (cm)
MAXIMUM CURRENT SPEED (cm/s) (DEPTH MEAN)
WIND SPEED (m/s) AT TIME OF MAX WAVE
CURRENT SPEED (cm/s) (DEPTH MEAN) AT TIME OF MAX WAVE
PEAK PERIOD (sec) AT TIME OF MAX WAVE (BY REGRESSION)

 Return    HSig     HMax   HCrest    maxWS maxHSUR    maxCS   assoWS   assoCS      TP(r)
             (m)      (m)      (m)    (m/s)    (cm)   (cm/s)   (m/s)   (cm/s)      (sec)

PercentMax: GUMBEL Distribution, Sector:   0.0 to 360.0 degrees

     1     0.90     1.71     1.26     0.00     0.0      0.0     0.00     0.0     3.5586
     5     1.47     2.89     1.96    20.30    75.6     42.3    20.21    39.2     4.6554
    10     1.64     3.21     2.18    22.56    90.8     48.1    22.48    45.1     4.9281
    25     1.85     3.61     2.45    25.41   106.1     55.0    25.32    51.9     5.2562
    50     2.00     3.92     2.66    27.53   116.8     60.0    27.42    56.8     5.4890
    53     2.01     3.94     2.67    27.70   117.7     60.5    27.60    57.2     5.5082
   100     2.15     4.22     2.86    29.62   127.2     65.0    29.50    61.5     5.7123
```

Figure 5. CASMOS sample extreme analysis results